

# A microstructural study on the high temperature oxidation, carburization and sulfidation of HK 40 and Incoloy 802

I. Caminha<sup>1</sup>, C. Barbosa<sup>1,2</sup>, I. Abud<sup>1</sup>, S. Santana de Carvalho<sup>1,2</sup>,  
F. C. de Souza Coelho dos Santos<sup>2</sup> & M. de Jesus Monteiro<sup>1</sup>

<sup>1</sup>Laboratory of Characterization of Mechanical and Microstructural Properties, National Institute of Technology (INT), Rio de Janeiro, Brazil

<sup>2</sup>Center of Characterization on Nanotechnology, National Institute of Technology (INT), Rio de Janeiro, Brazil

## Abstract

The main purpose of this article is an analysis of the microstructural changes in stainless steels and other special alloys due to high temperature phenomena, such as oxidation, carburization and sulfidation. These conditions arise in a plant during the production of polymeric materials, when the raw material, coke originating from petroleum, rich in carbon and sulfur, is in direct contact with tubes fabricated with metallic materials at elevated temperatures during the pyrolysis process. These changes can damage the characteristics and properties of the alloys, thus leading to premature failure in certain regions of the pipeline. In this work, techniques such as optical microscopy, field emission scanning electron microscopy (FESEM) equipped with an EDS microanalysis system and hardness tests were employed to analyze HK 40 stainless steel and Incoloy 802 used in pyrolysis tubes for polymeric material production. The presence of many undesirable oxide, carbide and sulfide particles and chromium depletion was identified mainly in the inner surface of the tubes in direct contact with the coke at elevated temperatures (around 1000°C). Variations of the corrosive attack were observed along different positions in the pipeline, depending on the more or less extensive exposure to high temperatures and corrosive agents. It can be concluded that the degradation which led to the premature failure of the pipeline



was caused by these microstructural changes in the alloys subjected to high temperature and contact with carbon and sulfur rich coke.

*Keywords: microstructure, microscopy, stainless steels, special alloys, high temperature degradation.*

## 1 Introduction

Heat resistant special alloys must present requirements of corrosion resistance and mechanical strength at high temperatures applications. However, when components fabricated with such materials work in very aggressive environments, the presence of harmful agents can degrade the microstructural characteristics and consequently their properties, favored by the acceleration and enhancement of diffusion of these deleterious atoms in such high temperatures [1–6].

In the production of polymeric materials, petroleum rich in carbon and sulfur is firstly converted in coke, where these elements remain and this raw material is subjected to high temperature conditions, around 1000°C, and transported through a pipeline usually fabricated with materials that present very high corrosion resistance, such as HK 40 stainless steel and Incoloy 802. In spite of these very good microstructural characteristics and chemical and mechanical properties, these materials can be attacked in very aggressive conditions. At this high temperature atomic diffusion is accelerated in such manner that oxygen atoms from the atmosphere and carbon and sulfur atoms from the coke can migrate into the metallic material, where it forms harmful compound such as oxides, carbides and sulfides, which cause many damages: loss of mass, degradation of toughness and corrosion resistance and eventually the collapse of the pipeline structure. Despite this catastrophic aspect, the degradation degree varies along the length of the pipeline: in some regions, where the conditions are still more aggressive (higher temperatures and/or more exposure to the aggressive elements, for instance), whereas in other regions these conditions are not as severe, and as consequence it is more intense in some regions than in other areas of the pipeline.

In this work, samples of pipelines fabricated with HK 40 stainless steel and Incoloy 802 nickel based superalloy were analyzed by optical microscopy (OM), field emission scanning electron microscopy (FESEM) and Vickers hardness tests. The results showed the presence of many undesirable oxide, carbide and sulfide particles, and chromium depletion was also identified, mainly in the inner surface of the tubes in direct contact with the coke at elevated temperatures (around 1000°C). Variations of the corrosive attack were observed along different positions in the pipeline, depending on the more or less extensive exposure to high temperatures and corrosive agents. Probably the premature failure of the pipeline was caused by these microstructural changes in the alloys subjected to high temperature and contact with carbon and sulfur rich coke.

## 2 Materials and methodology

Samples of stainless steel and superalloy used in the pyrolysis stage of polymeric materials fabrication are presented in figure 1. In this image sample 81 (mounted: left) and a sample of the inner surface of the tube (right) with greenish stains are displayed. Several similar samples were received and analyzed. Two types of metallic materials were used in the fabrication of the tubes: HK 40 stainless steels (25% Cr and 35% Ni) at the input of the system and Incoloy 802 (35% Cr and 45%Ni) at the output (higher temperatures: 35% Cr and 45%Ni) of the system.

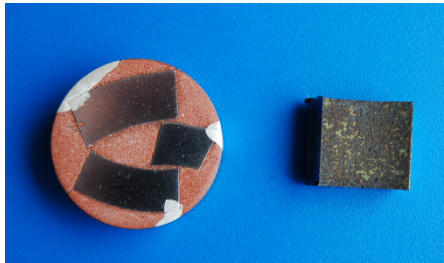


Figure 1: Samples: after metallographic preparation (left) and as received (right).

Failure occurred in different circumstances: while samples 74 and 76 presented normal lifetime (about 6 years), other samples (66, 70, 81, 82 and inner surface with greenish stains) were removed from tubes which showed premature failure (shorter life time, around 3 years). One of the samples (73) was removed from a nearly new tube, only as a reference for comparison. Sample 70 presented similar results to sample 66, as well as sample 76 with the same results of sample 74.

The chemical composition of the materials is presented in table 1.

Table 1: Nominal chemical composition: HK 40 stainless steel [7].

Element	C	Cr	Ni	Si	Fe
Mass %	0.35-0.45	23.0-27.0	19.0-22.0	1.75 max.	Balance

Table 2: Nominal chemical composition: Incoloy 802 [7].

Element	C	Cr	Ni	Si	Mn	Fe
Mass %	0.4	21.5	32.5	0.4	0.8	46.0

## 2.1 Metallographic analysis

The samples for metallographic analysis were subjected to the standard preparation method [8–9]. The HK 40 stainless steel samples were etched with a solution of 10 g oxalic acid in 100ml of distilled water at 6 V for 45 to 60 s, while the Incoloy 802 samples were etched with a solution of 70 ml H<sub>3</sub>PO<sub>4</sub> with 30 ml of distilled water, 5 to 10 V and 5 to 60 s.

## 2.2 Mechanical properties

Vickers hardness tests were performed with a 5 kgf (around 49 N) load according to NBR ISO 188-1:99 standard [10].

## 2.3 Field Emission Scanning Electron Microscopy (FESEM)

The same samples of the metallographic analysis and hardness tests were subjected to Field Emission Scanning Electron Microscopy (FESM). This equipment was operated at 20 kV and in the same equipment EDS (energy dispersion spectroscopy) was performed with the purpose of identifying different elements present in these alloys, although in a semi quantitative basis.

# 3 Results

## 3.1 Optical Microcopy (OM)

Figure 2 presents the microstructure of the sample 81 observed in an optical microscope, while figure 3 reveals details of the aspect of greenish stains in the inner surface of the pyrolysis tubes.

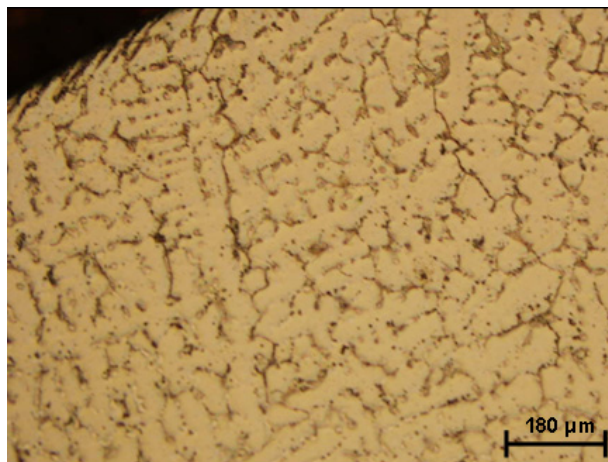


Figure 2: Microstructure of sample 81 (inner surface) – optical microscope.

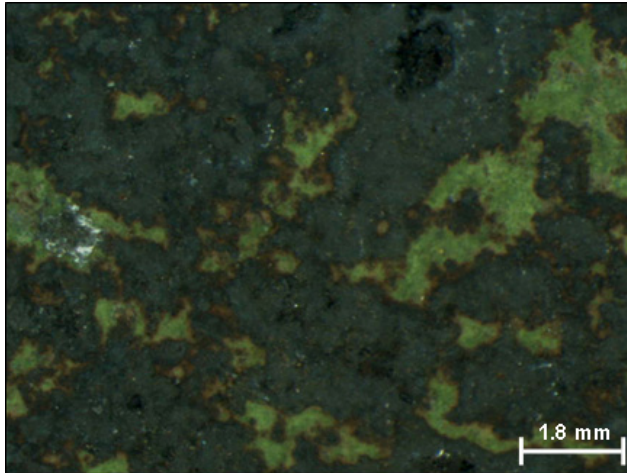


Figure 3: Inner surface of sample 81 with greenish stains: stereomicroscope.

### 3.2 Field Emission Scanning Electron Microscopy (FESEM)

Figure 4 shows the aspect of the microstructure of sample 66 observed in a field emission scanning electron microscope (FESEM) with backscattering electrons. Figure 5 presents the regions where EDS analysis was performed and the EDS spectrum corresponding to region 6.

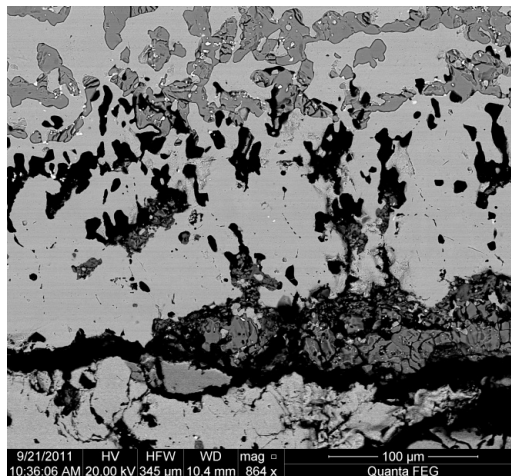


Figure 4: SEM BSE image sample 66 inner surface, output.

While Figures 4 and 5 refer to sample 66, the next images (Figures 6 and 7) show equivalent results for sample 82, and the following ones (Figures 8 and 9) for the inner surface of the same sample.

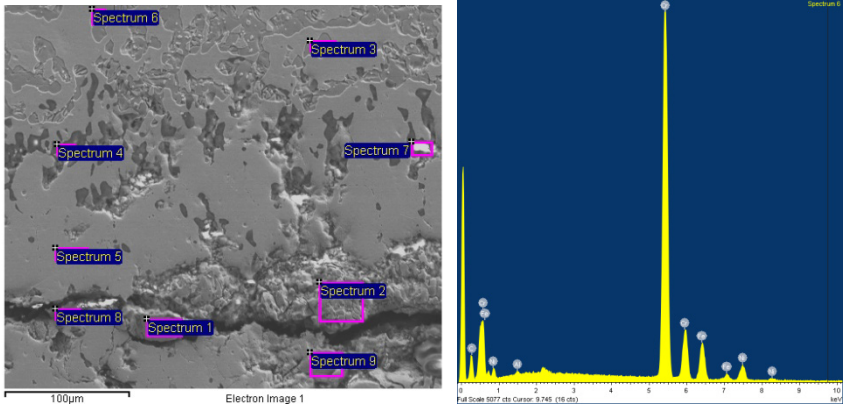


Figure 5: Regions selected for EDS analysis: sample 66 inner surface, output (left side) and EDS spectrum obtained from region 6 (right side).

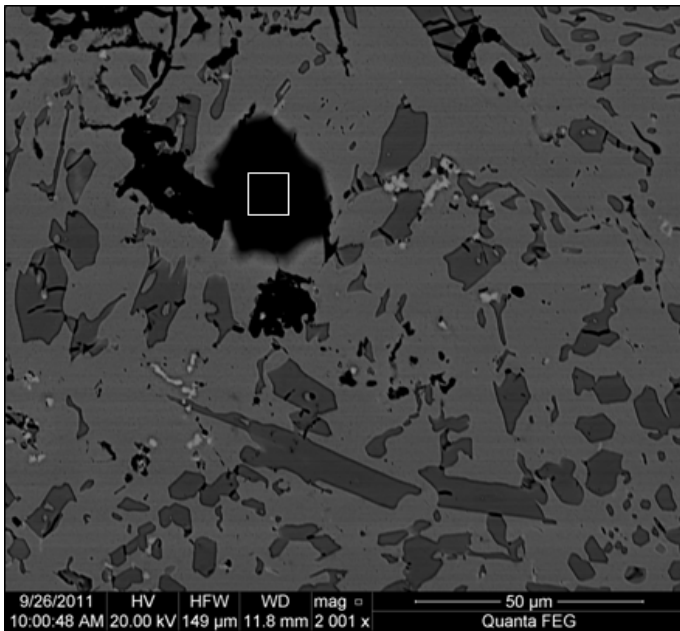


Figure 6: SEM backscattering electrons image of region with S rich particles. Region of sample 82 subjected to EDS analysis: indicated by a rectangle (inside).

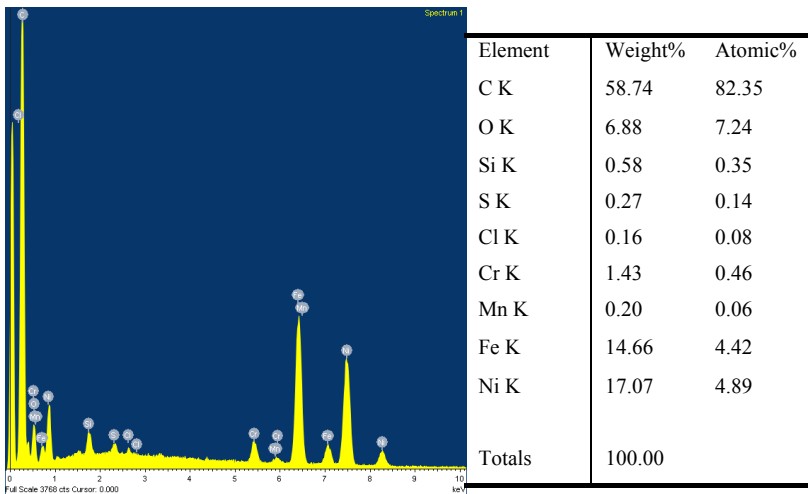


Figure 7: EDS spectrum analysis: S rich particles in the region indicated by rectangle Figure 6.

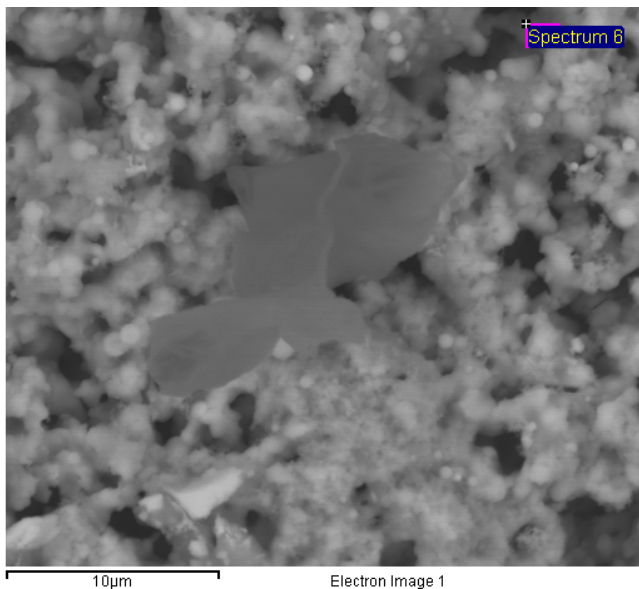
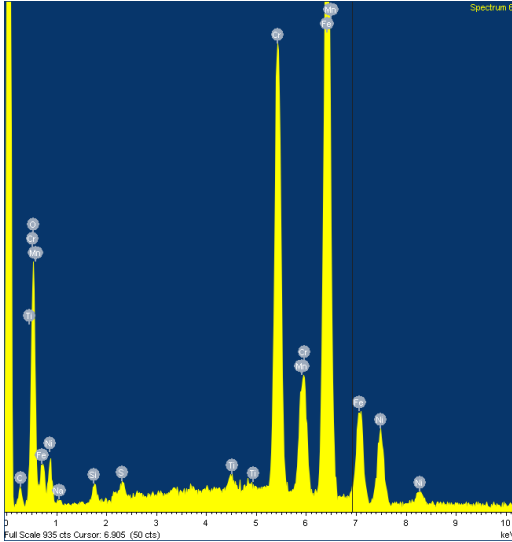


Figure 8: Sulfur rich particle in another region: inner surface of sample 82 with greenish stains.

Figure 9 shows the corresponding EDS microanalysis spectrum.

Figure 10 presents a SEM image with different layers forms the surface to the inner region of the sample and figure 11 the corresponding EDS microanalysis with C and Cr contents in each region.



Element	Weight%	Atomic%
C K	3.27	10.83
O K	10.39	25.85
Na K	0.36	0.63
Si K	0.44	0.63
S K	0.28	0.35
Ti K	0.32	0.27
Cr K	22.01	16.84
Mn K	4.71	3.41
Fe K	49.74	35.45
Ni K	8.47	5.74
Totals	100.00	

Figure 9: EDS spectrum obtained from region 6 (previous image in Figure 8): sample 82 surface with greenish stains.

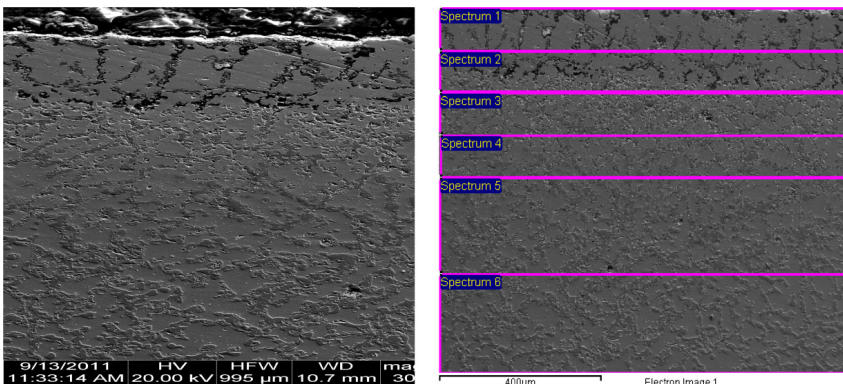


Figure 10: SEM image with different layers from the surface to the inner region of the sample 73 inner surface.

Spectrum	C	O	Al	Si	Cr	Mn	Fe	Ni	Nb	Total
1	4.80	12.46	0.36	4.32	18.28	0.69	15.86	43.22		100.00
2	7.08	8.54	0.29	3.88	21.77		15.86	42.59		100.00
3	9.94		0.31	0.59	34.22		14.85	38.06	2.02	100.00
4	9.86		0.25	0.85	34.39	0.66	14.43	38.09	1.47	100.00
5	10.61		0.23	1.03	36.74	0.73	13.75	35.64	1.28	100.00
6				1.44	39.96	1.00	15.50	40.61	1.49	100.00
Max.	10.61	12.46	0.36	4.32	39.96	1.00	15.86	43.22	2.02	
Min.	4.80	8.54	0.23	0.59	18.28	0.66	13.75	35.64	1.28	

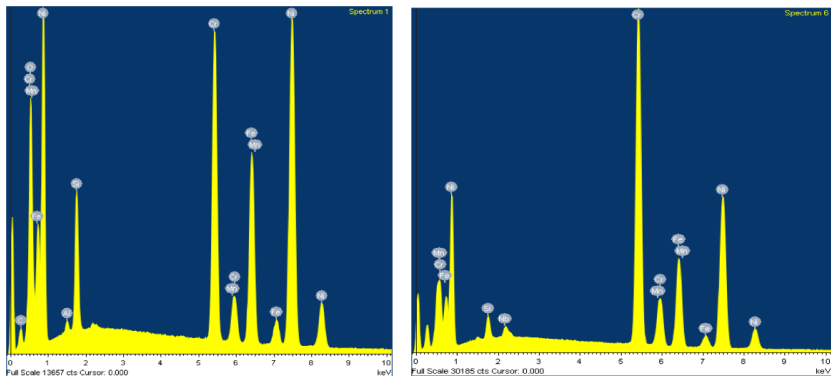


Figure 11: EDS microanalysis spectra, layers 1 (surface) and 6 (inner layer) from the sample 73-11-1P inner surface.

### 3.3 Hardness tests

Table 3 presents the hardness values of sample 73 inner surface (Vickers with 1 kgf or 9.8 N load: HV1), revealing the variation from the outer layer (1) to the inner layer (6). Five indentations were carried out on each layer.

Table 3: Vickers hardness (HV5) values of sample 73.

HV5	Points					
Layer (Spectrum)	1	2	3	4	5	Average
1	274.73	253.99	184.16	236.82	442.61	278.46
2	437.45	477.26	470.48	407.51	464.50	451.44
3	455.75	499.60	435.66	402.16	409.69	440.57
4	464.83	459.93	430.03	470.82	381.04	441.33
5	353.75	369.10	379.82	347.07	366.78	363.31
6	255.86	271.91	253.06	249.01	224.62	250.89

Based on standard deviation values (about 95% confidence) the variation of hardness with the layers is plotted in figure 8.

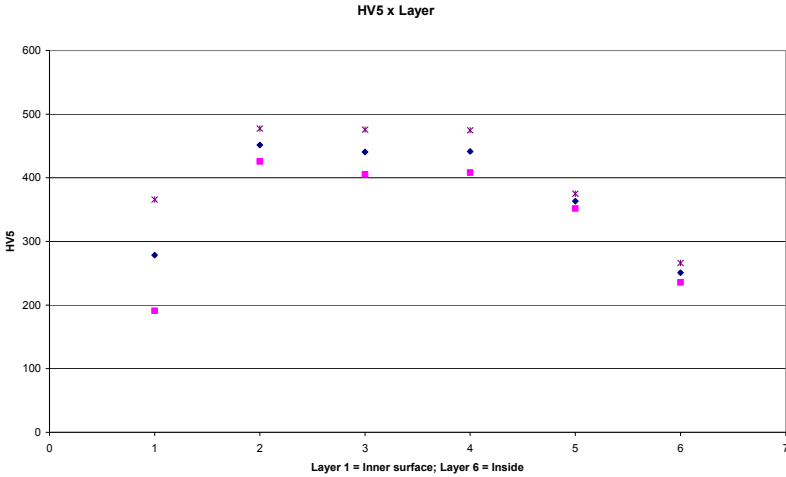


Figure 12: Hardness (HV5) variation along the 6 layers: 1 inner surface, 6: inside the tube.

This plot shows a clear tendency: the hardness of the inner surface (layer 1) is relatively low and when the distance to this surface increases the hardness value also increases. Then it reaches a steady level (layers 2 to 4) until at some distance it starts to diminish (layers 5 and 6), reaching on layer 6 a slightly harder value than layer 1.

#### 4 Discussion

The several results obtained in this work confirm that the problem in the tubes was associated to the formation of brittle particles and to the chromium depletion, since this element is responsible for the formation of a passive Cr<sub>2</sub>O<sub>3</sub> scale on the surface of the material, which provides corrosion resistance, mainly on the inner surface, subjected to contact with the coke formed during the pyrolysis process, earlier stage of the production of polymeric materials fabricated with petroleum as raw material.

In nearly all analyzed samples the chromium depletion was observed, from the middle region of the sample to its surface. As an example, in sample 73 (figure 11) the chromium content diminishes from 39.38% in the middle region to 18.28% in the surface, while in sample 74 it varied from 25.67 to 12.58% in the respective equivalent regions.

Several particles were observed and analyzed by an EDS device installed in the FESEM: mainly oxides, carbides and, in just some instances, sulfides (samples 66, 82 and inner surface with greenish stains, as shown in figures 5, 7 and 9, respectively). In these samples, and also in sample 81 (not shown in this paper), the presence of sodium (Na) was also identified.

Several carbide forming elements were identified, such as chromium, iron, niobium, titanium and silicon. Oxide forming elements were also found, such as chromium, iron, manganese and even aluminum. Sulfide particles are scarcer, as already mentioned, but in the regions where sulfur was identified, sulfide forming elements were also found, such as chromium, nickel, manganese, iron and sodium, but their presence cannot be considered negligible. Other less common elements were observed in some regions or particles, such as phosphor (P), brome (Br) and chlorine (Cl).

The technical literature reports the degradation of this type of material at high temperatures (around 1000°C), associated to the formation of carbides in carbon rich environments, which absorb mainly chromium (but also some other elements), which was present in the matrix and in the passive oxide scale, which rendered good corrosion resistance, thus favoring the progress of the corrosive process at high temperatures [1–2].

Hardness variation across the different layers of the material can be interpreted in this way: in the surface (layer 1) there are several cracks that affect the indentations. According to the literature [11], the propagation of cracks leads to energy release, thus lowering stress levels, which can contribute to hardness decrease. Therefore, it is not unexpected that hardness values are lower in this region than in other layers. In the following layers (2 to 4), placed more distant to the surface, hardness is kept in a higher level that nearly does not vary along these layers. It seems that the carbon enrichment in these layers can lead to the formation of carbides that can harden these layers, where cracks were not seen. In the fifth layer hardness starts to decrease. Probably in this region the distance to the surface is large enough to diminish the carbon enrichment and this tendency is still more evident in the sixth layer, the most distant from the surface, where the hardness is still lower, probably due to still lower carbon content.

## 5 Conclusion

- Degradation and premature failure of the tubes is associated to the formation of brittle particles and to the chromium depletion. This is the main element responsible for the formation of the passive scale which provides good corrosion resistance in these metallic materials. The chromium depletion is still more marked in the layers which are nearer to the surface, mainly in the inner surface which is in direct contact with coke formed during pyrolysis process.
- In all samples, which were analyzed in this study, the chromium depletion was observed to be stronger in the surface than in the inner regions of the sample.
- Among several particles found in these metallic materials oxides, carbides (of chromium, silicon, iron and manganese) and, in some samples, sulfides (of chromium, nickel, manganese, iron and sodium).
- In some regions the presence of sodium (Na), phosphor (P), bromine (BR) and chlorine (Cl) was identified.



## References

- [1] Luton, R.P.; Ramanarayan, T.A.; Mixed Oxidant Attack of High Temperature Alloys in carbon and Oxygen Containing Environments, *Oxidation of Metals*, 34, (5/6), 1990, 381-400.
- [2] Shi, S.; Lippold J.C.; Microstructure evolution during service exposure of two cast heat resisting stainless steels HP-Nb modified and 20-32 Nb, *Materials Characterization*, 59, 2008, 1029-1040.
- [3] Tjokro, K.; Young, D.J.; Johansson, R.E.; Ivarsson, B.G.; High temperature sulfidation oxidation of stainless steels, *Journal de Physique IV*, 3, 1993, 357-364.
- [4] Jakobi, D. (Schmidt + Clemens Group), S + C Spun casting, Failure Mechanisms for Radiant Tubes (Attack by Contaminants, e.g. Sodium), [www.schmidt-clemens](http://www.schmidt-clemens.com), 3 p.
- [5] Specs: 309/309S, 310/310S, Sandmeyer Steel Company, Philadelphia, PA, USA, [www.sandmeyersteel.com](http://www.sandmeyersteel.com), 7 p.
- [6] Sims, C.T.; Hagel, W.C.; “The Superalloys”, John Wiley & Sons, New York, 1972, p. 1- 565.
- [7] ASM Handbook, volume1, properties and selection: Irons, Steels and High performance Alloys, ASM International, Materials park, Ohio, USA, 1990 (2001), p.910-915.
- [8] ASTM E 3 Standard: “Standard Guide for Preparation of Metallographic Specimens”, 2011.
- [9] ASTM E 407 Standard: 407: “Standard Practice for Microetching Metals and Alloys”, 2007 (2011).
- [10] ISO 6507-1 Standard: “Metallic materials – Vickers hardness test – Part 1: Test method”, 2005.
- [11] Broek, D.; Elementary Engineering Fracture Mechanics, Kluwer Academic Publishers, 4th edition, Dordrecht, Netherlands, 1986 (2002), p.150-178.